Joint Beamforming Design for Double Active RIS-assisted Radar-Communication Coexistence

Mengyu Liu[1], Hong Ren[1], Cunhua Pan[1], Boshi Wang[1], Zhiyuan Yu[1], Ruisong Weng[1] and Kangda Zhi[2]
[1]Southeast University, Nanjing, China
[2]Queen Mary University of London, London, U.K.
Email: {mengyuliu, hren, cpan, 220230800, zyyu, 230239439}@seu.edu.cn, k.zhi@qmul.ac.uk

2024 IEEE International Workshop on Radio Frequency and Antenna Technologies (iWRF&AT) | 979-8-3503-8476-5/24/$31.00 ©2024 IEEE | DOI: 10.1109/iWRFAT61200.2024.10594442

***Abstract*—In this paper, we consider a double active RIS-assisted RCC system, which focuses on the design of the radar's beamforming vector and the active RISs' reflecting coefficient matrices, to maximize the achievable data rate of the communication system. The considered system needs to meet the radar detection constraint and the power budgets at the radar and the RISs. Since the problem is non-convex, we propose an algorithm based on penalty dual decomposition (PDD) framework. Specifically, we initially introduce auxiliary variables to reformulate the coupled variables into equation constraints and incorporating these constraints into the objective function through the PDD framework. Then, we decouple the equivalent problem into several subproblems by invoking block coordinate descent (BCD) method. Furthermore, we employ the Lagrange dual method to alternately optimize these subproblems. Simulation results verify that under the same power budget, deploying double active RISs in RCC system can achieve higher system performance compared with single active RIS and double passive RISs.**

***Index Terms*—Active reconfigurable intelligent surface (RIS), integrated sensing and communication (ISAC), radar-communication coexistence (RCC), penalty dual decomposition (PDD) algorithm.**

I. INTRODUCTION

Integrated sensing and communication (ISAC) technology can integrate the communication system and radar system by sharing frequency band resources, transmission waveforms, and hardware platforms. There are two main implementation approaches for ISAC [1]: the radar-communication coexistence (RCC) system and the dual-functional radar and communication (DFRC) system. For the former, the hardware parts of the radar and the communication system are separate [2], while for the latter, the hardware parts of the radar and the communication system are integrated [1]. Compared with DFRC systems, RCC systems typically refrain from altering the existing hardware structure and only consider the design of resource allocation strategies. With this in mind, RCC systems have attracted considerable interest [3]. However, the interference between radar and communication equipment can seriously degrade the achievable data rate of the communication system. To solve this issue, some works have deployed reconfigurable intelligent surface (RIS) in RCC systems to eliminate the interference between the communication systems and the radar [4], [5]. Specifically, RISs are endowed with the ability to customize the wireless channel and thus enhance the signal transmission [6].

However, the system performance gain from deploying RIS is limited by the effect of "multiplicative fading" [7]. Fortunately, the concept of active RIS is proposed to overcome these limitations [7], [8]. Different from passive RIS, active RIS is equipped with an integrated active amplifier on each reflective element to compensate for signal attenuation, so that the gain of RIS can be fully unleashed. Motivated by this, researchers have introduced active RIS into DFRC systems [9], [10]. In [9], an active RIS was deployed in DFRC system to enhance radar sensing performance and communication quality. Additionally, in [10], active RIS has been applied to improve physical layer security in DFRC systems. These literatures validated the superiority of active RIS over passive RIS in DFRC systems. However, these works mainly focused on DFRC scenarios with a single active RIS. To the best of the authors' knowledge, the active RIS-aided RCC systems have not been studied, which is also an important application scenario for ISAC. Besides, considering the promising cooperative gain between double RISs, the investigation of double active RISs-aided RCC systems is of significant importance, and it is expected to achieve superior performance.

In this paper, we investigate a double active RIS-assisted RCC system. Due to the incorporation of active RIS, the power constraints of active RIS need to be considered, which means that the methods proposed by [4] and [5] cannot be directly applied. Meanwhile, the deployment of double RISs also introduces non-trivial challenges for the beamforming design. To tackle these challenges, we propose a low-complexity algorithm to solve the formulated optimization problem.

II. SYSTEM MODEL AND PROBLEM FORMULATION

As shown in Fig. 1, we consider a double active RIS-assisted RCC system[1], which consists of a pair of single-antenna base station (BS) and single-antenna user (UE) and a multiple-input multiple-output (MIMO) radar with M antennas. Additionally, two active RISs named as active RIS 1 and active RIS 2 are equipped with N_1 and N_2 reflecting elements, respectively.

[1]We assume that the BS, radar and two RISs are all connected to the same central controller, which provides the channel state information (CSI). The required CSI can be obtained by some efficient channel estimation algorithms [11], [12].

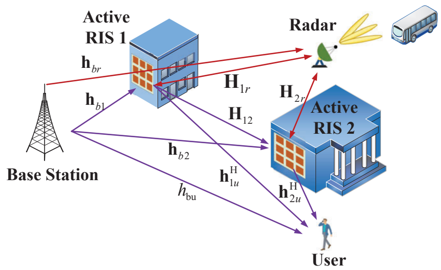

Fig. 1. Double active RIS-assisted radar-communication coexistence system.

A. Radar Model

We assume that the radar mainly detects potential targets in some directions. The K directions during one detection epoch are given by $\{\theta_k\}, \forall k \in \mathcal{K} \triangleq \{1, 2, \cdots, K\}$. T is used to represent the pulse repetition interval (PRI). In addition, we assume that the the probing signal is transmitted by radar at time t, and the echo signal is received from the targets at time t_0. Therefore, the probing signal transmitted by radar can be regarded as

$$\mathbf{x}[t] = \begin{cases} \mathbf{w}_k s_k, & t = (k-1)T, \forall k \in \mathcal{K}, \\ \mathbf{0}, & t \neq (k-1)T, \forall k \in \mathcal{K}. \end{cases} \tag{1}$$

where s_k and $\mathbf{w}_k \in \mathbb{C}^{M \times 1}$ denote the radar sensing symbols and the transmitting beamforming vector for direction $\theta_k, \forall k \in \mathcal{K}$, respectively. Specifically, we assume s_k is an independent Gaussian random symbol with zero mean and unit signal power.

Let $\mathbf{h}_{br} \in \mathbb{C}^{M \times 1}$, $\mathbf{h}_{b1} \in \mathbb{C}^{N_1 \times 1}$, $\mathbf{H}_{1r} \in \mathbb{C}^{M \times N_1}$ and $\mathbf{H}_{2r} \in \mathbb{C}^{M \times N_2}$ denote the wireless channel for BS-radar, BS-active RIS 1, active RIS 1-radar, active RIS2-radar, respectively. Specifically, $\rho_{i,n_i} e^{\varphi_{i,n_i}}$ denotes the reflecting coefficient of the n-th reflecting element of the i-th active RIS, where $\rho_{i,n_i} > 1$ and $\varphi_{i,n_i} \in [0, 2\pi]$. Then, the reflecting coefficient matrix of the i-th active RIS is $\mathbf{\Theta}_i = \mathrm{diag}(\boldsymbol{\phi}_\mathrm{i})$, where $\boldsymbol{\phi}_i \triangleq [\rho_{i,1_i} e^{\varphi_{i,1_i}}, \cdots, \rho_{i,N_i} e^{\varphi_{i,N_i}}]^\mathrm{T}, i \in \{1, 2\}$.

The received signal by radar from the target in θ_k can be expressed as (2), as shown at the bottom of this page, where $\mathbf{A}_k \triangleq \alpha_k \mathbf{a}(\theta_k) \mathbf{a}^\mathrm{H}(\theta_k) \in \mathbb{C}^{M \times M}$ is the target response matrix for the direction θ_k, α_k denote the pathloss factor from direction θ_k and $\mathbf{a}(\theta_k) \triangleq \left[1, e^{j\frac{2\pi d}{\lambda}\sin\theta_k}, \cdots, e^{j\frac{2\pi d}{\lambda}(M-1)\sin\theta_k}\right]^\mathrm{T}$ as the array response vector, where d and λ denote the antenna spacing and the signal wavelength, respectively. Moreover, $\mathbf{n}[t] \sim \mathcal{CN}\left(\mathbf{0}, \sigma^2 \mathbf{I}_M\right)$ denote the thermal noise at radar.

Furthermore, $\mathbf{d}_k^\mathrm{H} \in \mathbb{C}^{1 \times M}$ is the receive beamforming vector for the direction θ_k. Thus, by defining the equivalent channel matrices $\mathbf{B} \triangleq \mathbf{H}_{2r}\mathbf{\Theta}_2\mathbf{H}_{12}\mathbf{\Theta}_1 + \mathbf{H}_{1r}\mathbf{\Theta}_1 \in \mathbb{C}^{M \times N_1}$, $\mathbf{C} \triangleq \mathbf{H}_{2r}\mathbf{\Theta}_2 \in \mathbb{C}^{M \times N_2}$, $\mathbf{q} \triangleq \mathbf{h}_{br} + \mathbf{B}\mathbf{h}_{b1} + \mathbf{C}\mathbf{h}_{b2} \in \mathbb{C}^{M \times 1}$, the radar SINR for the direction θ_k can be expressed as (3), as shown at the bottom of this page.

B. Communication Model

Let h_{bu}, $\mathbf{h}_{b1} \in \mathbb{C}^{N_1 \times 1}$, $\mathbf{h}_{b2} \in \mathbb{C}^{N_2 \times 1}$, $\mathbf{H}_{12} \in \mathbb{C}^{N_2 \times N_1}$, $\mathbf{h}_{2u}^\mathrm{H} \in \mathbb{C}^{1 \times N_2}$, $\mathbf{h}_{1u}^\mathrm{H} \in \mathbb{C}^{1 \times N_1}$ denote the wireless channel for BS-UE, BS-active RIS 1, active RIS 1-active RIS 2, active RIS 2-UE, active RIS 1-UE, respectively. Therefore, the received signal at the user at the time t can be expressed as (4), as shown at the bottom of next page, where $c[t]$ and P_t^a denote the communication signal from BS and the transmitted power at BS. $n_0[t] \sim \mathcal{CN}\left(0, \sigma_0^2\right)$ and $\mathbf{n}_i[t] \sim \mathcal{CN}\left(\mathbf{0}, \sigma_i^2 \mathbf{I}_{Ni}\right)$ are the thermal noise at the user and the i-th active RIS, respectively.

Note that, as shown in Fig. 1, the targets are not located near active RIS and active RIS is usually deployed on the side of buildings. Moreover, when the number of radar antennas is large, the radar beam is usually narrow, making it less likely to interfere with the communication system. Therefore, the interference from radar to user is small and can be ignored[2].

The communication SNR for the user during one detection epoch can be expressed as (5), as shown at the bottom of next page. Then, the achievable data rate (bit/s/Hz) is given by

$$R = \log_2(1 + \mathrm{SNR}^\mathrm{c}). \tag{6}$$

Furthermore, since the active RIS is equipped with integrated active amplifiers [7], the power constraints of active RIS 1 and active RIS 2 can be expressed as follows

$$\|\mathbf{\Theta}_1\mathbf{h}_{b1}\|_2^2 + \sigma_1^2\|\mathbf{\Theta}_1\|_F^2 \leq P_1, \tag{7a}$$
$$\|\mathbf{\Theta}_2\mathbf{H}_{12}\mathbf{\Theta}_1\mathbf{h}_{b1}\|_2^2 + \|\mathbf{\Theta}_2\mathbf{h}_{b2}\|_2^2 + \sigma_1^2\|\mathbf{\Theta}_2\mathbf{H}_{12}\mathbf{\Theta}_1\|_F^2$$

[2] The interference from radar to user can also be reduced using some techniques in [13], [14].

$$\begin{aligned} \mathbf{y}_k^\mathrm{r}[t] = & \underbrace{\mathbf{A}_k\mathbf{x}[t-t_0]}_{\text{Echo signal from the target}} + \underbrace{(\mathbf{H}_{1r}\mathbf{\Theta}_1 + \mathbf{H}_{2r}\mathbf{\Theta}_2\mathbf{H}_{12}\mathbf{\Theta}_1)\mathbf{n}_1[t] + \mathbf{H}_{2r}\mathbf{\Theta}_2\mathbf{n}_2[t] + \mathbf{n}[t]}_{\text{Thermal nosie}} \\ & + \underbrace{\sum_{m=1, m\neq k}^{K} \mathbf{A}_m\mathbf{x}[t-t_0]}_{\text{Interference from other targets}} + \underbrace{(\mathbf{h}_{br} + \mathbf{H}_{1r}\mathbf{\Theta}_1\mathbf{h}_{b1} + \mathbf{H}_{2r}\mathbf{\Theta}_2\mathbf{h}_{b2} + \mathbf{H}_{2r}\mathbf{\Theta}_2\mathbf{H}_{12}\mathbf{\Theta}_1\mathbf{h}_{b1})\sqrt{P_\mathrm{t}^\mathrm{a}}c[t]}_{\text{Interference from BS to radar}} \end{aligned} \tag{2}$$

$$\mathrm{SINR}_k^\mathrm{r} = \frac{\left|\mathbf{d}_k^\mathrm{H}\mathbf{A}_k\mathbf{w}_k\right|^2}{\sum\limits_{m=1, m\neq k}^{K} \left|\mathbf{d}_k^\mathrm{H}\mathbf{A}_m\mathbf{w}_k\right|^2 + P_\mathrm{t}^\mathrm{a}\left|\mathbf{d}_k^\mathrm{H}\mathbf{q}\right|^2 + \sigma_1^2\left\|\mathbf{d}_k^\mathrm{H}\mathbf{B}\right\|_2^2 + \sigma_2^2\left\|\mathbf{d}_k^\mathrm{H}\mathbf{C}\right\|_2^2 + \sigma^2\left\|\mathbf{d}_k^\mathrm{H}\right\|_2^2} \tag{3}$$

$$+\sigma_2^2\|\boldsymbol{\Theta}_2\|_F^2 \leq P_2, \quad (7b)$$

where P_1 and P_2 denote the power budgets of active RIS 1 and active RIS 2, respectively.

C. Problem Formulation

In this paper, we aim to maximize the achievable data rate of the communication system by jointly optimizing the transmit beamforming vector $\{\mathbf{w}_k\}$, receive beamforming vector $\{\mathbf{d}_k\}$ at the radar and the reflecting coefficient matrices $\boldsymbol{\Theta}_1$ and $\boldsymbol{\Theta}_2$ of active RISs while guaranteeing SINR of radar for each detecting direction $\{\theta_k\}$ and power limitation of radar and active RISs. For this single user system, maximizing the user's achievable rate is equivalent to maximizing the user's SNR. Hence, the optimization problem is formulated as

$$\mathcal{P}_1: \max_{\{\mathbf{w}_k\},\{\mathbf{d}_k\},\boldsymbol{\Theta}_1,\boldsymbol{\Theta}_2} \quad \mathrm{SNR}^{\mathrm{c}} \quad (8a)$$

$$\text{s.t.} \quad \mathrm{SINR}_k^{\mathrm{r}} \geq \eta, \forall k \in \mathcal{K}, \quad (8b)$$

$$\sum_{k=1}^{K}\|\mathbf{w}_k\|_2^2 \leq P_{\mathrm{r}}, \quad (8c)$$

$$\text{(7a), (7b),}$$

where η and P_{r} denote the SINR requirement and the power budget for the radar, respectively. Constraint (8b) denotes the minimum SINR requirement to ensure the detection accuracy of radar. Constraint (8c) shows the power budget of radar.

III. Algorithm

In this section, we first reformulate the original problem by using fractional programming (FP) method. Then, we apply this problem into the penalty dual decomposition (PDD) framework. Finally, the block coordinate descent (BCD) algorithm is used to obtain the optimal solution of each variable.

A. Reformulation of the Original Problem

Firstly, we introduce an auxiliary x and apply the FP method [15]. Then, the original objective function can be rewritten as

$$\tilde{f}(\boldsymbol{\Theta}_1,\boldsymbol{\Theta}_2,x) \triangleq |x|^2\left(\sigma_1^2\left\|\mathbf{h}_{2u}^{\mathrm{H}}\boldsymbol{\Theta}_2\mathbf{H}_{12}\boldsymbol{\Theta}_1+\mathbf{h}_{1u}^{\mathrm{H}}\boldsymbol{\Theta}_1\right\|_2^2 + \sigma_2^2\left\|\mathbf{h}_{2u}^{\mathrm{H}}\boldsymbol{\Theta}_2\right\|_2^2+\sigma_0^2\right) - 2\mathrm{Re}\{x^*\sqrt{P_{\mathrm{t}}^{\mathrm{a}}}(h_{\mathrm{bu}}+\mathbf{h}_{1u}^{\mathrm{H}}\boldsymbol{\Theta}_1\mathbf{h}_{b1} + \mathbf{h}_{2u}^{\mathrm{H}}\boldsymbol{\Theta}_2\mathbf{H}_{12}\boldsymbol{\Theta}_1\mathbf{h}_{b1}+\mathbf{h}_{2u}^{\mathrm{H}}\boldsymbol{\Theta}_2\mathbf{h}_{b2})\}, \quad (9)$$

where x^{opt} is represented by (10), shown at the bottom of this page.

B. The PDD Algorithm for the Outer Loop

By introducing the auxiliary variables $\{u_k, v_k, y_k, \mathbf{e}_k, \mathbf{t}_k\}$, the equality constraints associated with five auxiliary variables are as follows

$$u_k=\mathbf{d}_k^{\mathrm{H}}\mathbf{A}_k\mathbf{w}_k, v_k=\mathbf{d}_k^{\mathrm{H}}\mathbf{q}, \mathbf{e}_k^{\mathrm{H}}=\mathbf{d}_k^{\mathrm{H}}\mathbf{B}, \forall k\in\mathcal{K}, \quad (11a)$$

$$\mathbf{t}_k^{\mathrm{H}}=\mathbf{d}_k^{\mathrm{H}}\mathbf{C}, y_k=\sum_{m=1,m\neq k}^{K}\mathbf{d}_k^{\mathrm{H}}\mathbf{A}_m\mathbf{w}_k, \forall k\in\mathcal{K}. \quad (11b)$$

Next, we substitute the auxiliary variables into constraint (8b). The new constraint (8b) can therefore be written as

$$f(\mathbf{d}_k,v_k,y_k,\mathbf{e}_k,\mathbf{t}_k)-g(u_k)\leq 0, \forall k\in\mathcal{K}, \quad (12)$$

where $f(\mathbf{d}_k,v_k,y_k,\mathbf{e}_k,\mathbf{t}_k)=\eta(|y_k|^2+P_{\mathrm{t}}^{\mathrm{a}}|v_k|^2+\sigma_1^2\left\|\mathbf{e}_k^{\mathrm{H}}\right\|_2^2+\sigma_2^2\left\|\mathbf{t}_k^{\mathrm{H}}\right\|_2^2+\sigma^2\left\|\mathbf{d}_k^{\mathrm{H}}\right\|_2^2)$, $g(u_k)=|u_k|^2$. However, the constraint (12) is not convex, so we use the concave-convex procedure (CCP) method to solve this issue [16]. Thus, we approximate $g(u_k)$ in the i-th iteration by a first-order Taylor expansion near the point $u_k^{(i)}$, as $\hat{g}(u_k^{(i)},u_k)=2\mathrm{Re}((u_k^{(i)})^*u_k)-\left|u_k^{(i)}\right|^2$. Therefore, the constraint (12) can be rewritten as

$$f(\mathbf{d}_k,v_k,y_k,\mathbf{e}_k,\mathbf{t}_k)-\hat{g}(u_k^{(i)},u_k)\leq 0, \forall k\in\mathcal{K}. \quad (13)$$

Then, by applying the PDD framework [17], we can get the following new optimization problem

$$\mathcal{P}_2: \min_{\boldsymbol{\Omega}_1} \quad \tilde{f}(\boldsymbol{\Theta}_1,\boldsymbol{\Theta}_2,x)+\frac{1}{2\rho}\sum_{k=1}^{K}\left|u_k-\mathbf{d}_k^{\mathrm{H}}\mathbf{A}_k\mathbf{w}_k+\rho\lambda_{k,1}\right|^2 + \frac{1}{2\rho}\sum_{k=1}^{K}\left|v_k-\mathbf{d}_k^{\mathrm{H}}\mathbf{q}+\rho\lambda_{k,2}\right|^2 + \frac{1}{2\rho}\sum_{k=1}^{K}\left|y_k-\mathbf{d}_k^{\mathrm{H}}\mathbf{A}_m\mathbf{w}_k+\rho\lambda_{k,3}\right|^2 + \frac{1}{2\rho}\sum_{k=1}^{K}\|\mathbf{e}_k^{\mathrm{H}}-\mathbf{d}_k^{\mathrm{H}}\mathbf{B}+\rho\boldsymbol{\lambda}_{k,\mathrm{e}}^{\mathrm{T}}\|_2^2$$

$$\mathrm{y}^{\mathrm{c}}[t]=\underbrace{(h_{\mathrm{bu}}+\mathbf{h}_{2u}^{\mathrm{H}}\boldsymbol{\Theta}_2\mathbf{H}_{12}\boldsymbol{\Theta}_1\mathbf{h}_{b1}+\mathbf{h}_{1u}^{\mathrm{H}}\boldsymbol{\Theta}_1\mathbf{h}_{b1}+\mathbf{h}_{2u}^{\mathrm{H}}\boldsymbol{\Theta}_2\mathbf{h}_{b2})\sqrt{P_{\mathrm{t}}^{\mathrm{a}}}c[t]}_{\text{Communication signal from BS to user}} + \underbrace{(\mathbf{h}_{2u}^{\mathrm{H}}\boldsymbol{\Theta}_2\mathbf{H}_{12}\boldsymbol{\Theta}_1+\mathbf{h}_{1u}^{\mathrm{H}}\boldsymbol{\Theta}_1)\mathbf{n}_1[t]+\mathbf{h}_{2u}^{\mathrm{H}}\boldsymbol{\Theta}_2\mathbf{n}_2[t]+n_0[t]}_{\text{Thermal noise}} + \underbrace{((\mathbf{h}_{2u}^{\mathrm{H}}\boldsymbol{\Theta}_2\mathbf{H}_{12}+\mathbf{h}_{1u}^{\mathrm{H}})\boldsymbol{\Theta}_1\mathbf{H}_{1r}^{\mathrm{H}}+\mathbf{h}_{2u}^{\mathrm{H}}\boldsymbol{\Theta}_2\mathbf{H}_{2r}^{\mathrm{H}})\mathbf{x}[t]}_{\text{Interference from radar to user}} \quad (4)$$

$$\mathrm{SNR}^{\mathrm{c}}=\frac{P_{\mathrm{t}}^{\mathrm{a}}\left|h_{\mathrm{bu}}+\mathbf{h}_{2u}^{\mathrm{H}}\boldsymbol{\Theta}_2\mathbf{H}_{12}\boldsymbol{\Theta}_1\mathbf{h}_{b1}+\mathbf{h}_{1u}^{\mathrm{H}}\boldsymbol{\Theta}_1\mathbf{h}_{b1}+\mathbf{h}_{2u}^{\mathrm{H}}\boldsymbol{\Theta}_2\mathbf{h}_{b2}\right|^2}{\sigma_1^2\left\|\mathbf{h}_{2u}^{\mathrm{H}}\boldsymbol{\Theta}_2\mathbf{H}_{12}\boldsymbol{\Theta}_1+\mathbf{h}_{1u}^{\mathrm{H}}\boldsymbol{\Theta}_1\right\|_2^2+\sigma_2^2\left\|\mathbf{h}_{2u}^{\mathrm{H}}\boldsymbol{\Theta}_2\right\|_2^2+\sigma_0^2} \quad (5)$$

$$x^{\mathrm{opt}}=\frac{\sqrt{P_{\mathrm{t}}^{\mathrm{a}}}(h_{bu}+\mathbf{h}_{2u}^{\mathrm{H}}\boldsymbol{\Theta}_2\mathbf{H}_{12}\boldsymbol{\Theta}_1\mathbf{h}_{b1}+\mathbf{h}_{1u}^{\mathrm{H}}\boldsymbol{\Theta}_1\mathbf{h}_{b1}+\mathbf{h}_{2u}^{\mathrm{H}}\boldsymbol{\Theta}_2\mathbf{h}_{b2})}{\sigma_1^2(\left\|\mathbf{h}_{2u}^{\mathrm{H}}\boldsymbol{\Theta}_2\mathbf{H}_{12}\boldsymbol{\Theta}_1+\mathbf{h}_{1u}^{\mathrm{H}}\boldsymbol{\Theta}_1\right\|_2^2)+\sigma_2^2\left\|\mathbf{h}_{2u}^{\mathrm{H}}\boldsymbol{\Theta}_2\right\|_2^2+\sigma_0^2} \quad (10)$$

$$+\frac{1}{2\rho}\sum_{k=1}^{K}\|\mathbf{t}_k^{\rm H}-\mathbf{d}_k^{\rm H}\mathbf{C}+\rho\boldsymbol{\lambda}_{k,\rm t}^{\rm T}\|_2^2, \tag{14}$$

$$\text{s.t.} \quad (7a), (7b), (8c), (13),$$

where the set $\mathbf{\Omega}_1 \triangleq \{\mathbf{w}_k, \mathbf{d}_k, \mathbf{\Theta}_1, \mathbf{\Theta}_2, x, u_k, v_k, y_k, \mathbf{e}_k, \mathbf{t}_k\}$. ρ is the penalty parameter, $\{\lambda_{k,1}, \lambda_{k,2}, \lambda_{k,3}, \boldsymbol{\lambda}_{k,\rm e}^{\rm T}\boldsymbol{\lambda}_{k,\rm t}^{\rm T}\}$ are the dual parameters. When $\rho \to 0$, the solutions of problem $\mathcal{P}_2$ are equal to the problem $\mathcal{P}_1$. Additionally, the convergence of the PDD algorithm has been proved in [17]. The detailed algorithmic process can be seen in Algorithm 1.

Algorithm 1 PDD Algorithm

---

1. Initial the iteration number $t=0$, the tolerance of accuracy ε, $\rho^{(0)}>0$, $\sigma>0$, $0<c<1$. $\boldsymbol{\lambda}^{(0)}$ is the collection of dual parameters $\{\lambda_{k,2}^{(0)}, \lambda_{k,m,3}^{(0)}, \boldsymbol{\lambda}_{k,\rm e}^{\rm T(0)}, \boldsymbol{\lambda}_{k,\rm t}^{\rm T(0)}\}$. $\mathbf{h}^{(0)}$ is the collection of the deviation of the equality constraints (11a), (11b).
2. **repeat**
3. $\quad\mathbf{\Omega}_1^{(t+1)} = \text{optimize } \mathcal{P}_2(\mathbf{\Omega}_1^{(t)}, \rho^{(t)}, \boldsymbol{\lambda}^{(t)})$;
4. $\quad$Compute the deviation of the equality constraints $\mathbf{h}^{(t+1)}$;
5. $\quad$**if** $||\mathbf{h}^{(t+1)}||_\infty \le \sigma$ **then**
6. $\quad\quad\boldsymbol{\lambda}^{(t+1)} = \boldsymbol{\lambda}^{(t)} + \frac{1}{\rho^{(t)}}\mathbf{h}^{(t+1)}$, $\rho^{(t+1)} = \rho^{(t)}$;
7. $\quad$**else**
8. $\quad\quad\boldsymbol{\lambda}^{(t+1)} = \boldsymbol{\lambda}^{(t)}$, $\rho^{(t+1)} = c\rho^{(t)}$;
9. $\quad$**end if**
10. $\quad t = t+1$;
11. **until** $\frac{\left|\mathcal{P}_2(\mathbf{\Omega}_1^{(t+1)}, \rho^{(t+1)}, \lambda^{(t)+1}) - \mathcal{P}_2(\mathbf{\Omega}_1^{(t)}, \rho^{(t)}, \lambda^{(t)})\right|}{\mathcal{P}_2(\mathbf{\Omega}_1^{(t)}, \rho^{(t)}, \lambda^{(t)})} \le \varepsilon$

C. The BCD Algorithm for the Inner Loop

In this subsection, we solve the augmented Lagrange (AL) problem using the BCD method [18].

1) Optimizing the Beamforming Vector $\mathbf{w}_k$: In this subproblem, we fix other variables to optimize $\mathbf{w}_k$. We first define the following parameters

$$\mathbf{\Gamma}_k = \mathbf{A}_k^{\rm H}\mathbf{d}_k\mathbf{d}_k^{\rm H}\mathbf{A}_k + \sum_{m=1,m\neq k}^{K}\mathbf{A}_m^{\rm H}\mathbf{d}_k\mathbf{d}_k^{\rm H}\mathbf{A}_m, \tag{15a}$$

$$\mathbf{p}_k = (u_k+\rho\lambda_{k,1})\mathbf{A}_k^{\rm H}\mathbf{d}_k + (y_k+\rho\lambda_{k,3})\mathbf{A}_m^{\rm H}\mathbf{d}_k, \tag{15b}$$

$$\mathbf{\Gamma} = \text{blkdiag}([\mathbf{\Gamma}_1, \cdots, \mathbf{\Gamma}_K]), \mathbf{p} = [\mathbf{p}_1^{\rm T}, \cdots, \mathbf{p}_K^{\rm T}]^{\rm T}. \tag{15c}$$

Then, the Problem (14) can be reformulated as

$$\min_{\mathbf{w}} \quad \mathbf{w}^{\rm H}\mathbf{\Gamma}\mathbf{w} - 2\text{Re}\left\{\mathbf{p}^{\rm H}\mathbf{w}\right\}, \tag{16a}$$

$$\text{s.t.} \quad \mathbf{w}^{\rm H}\mathbf{w} \le P_{\rm r}, \tag{16b}$$

where we define $\mathbf{w} = [\mathbf{w}_1^{\rm T}, \cdots, \mathbf{w}_K^{\rm T}]^{\rm T}$. Then, we can use the Lagrange multiplier method [**?**] to solve this problem. $\mathbf{w}^{\rm opt}$ can be given by

$$\mathbf{w}^{\rm opt} = (\mathbf{\Gamma} + \mu\mathbf{I})^{-1}\mathbf{p}, \tag{17}$$

where $\mu \ge 0$ is the Lagrange multiplier associated with constraint (16b). The optimal value of μ can be determined by the bisection search method.

2) Optimizing the Receving Beamforming Vector $\mathbf{d}_k$: In this subproblem, we optimize $\mathbf{d}_k$ by fixing other variables. We first define the following parameters

$$\beth_k = \mathbf{A}_k\mathbf{w}_k\mathbf{w}_k{}^{\rm H}\mathbf{A}_k^{\rm H} + \sum_{m=1,m\neq k}^{K}\mathbf{A}_m\mathbf{w}_k\mathbf{w}_k^{\rm H}\mathbf{A}_m^{\rm H}$$
$$+\mathbf{q}\mathbf{q}^{\rm H} + \mathbf{B}\mathbf{B}^{\rm H} + +\mathbf{C}\mathbf{C}^{\rm H}, \tag{18a}$$

$$m = f(\mathbf{d}_k, v_k, y_k, \mathbf{e}_k, \mathbf{t}_k) - \hat{g}(u_k^{(i)}, u_k), \tag{18b}$$

$$\mathbf{z}_k = (u_k+\rho\lambda_{k,1})\mathbf{A}_k\mathbf{w}_k + (v_k+\rho\lambda_{k,2})\mathbf{q} + \mathbf{C}(\mathbf{t}_k^{\rm H}+\rho\boldsymbol{\lambda}_{k,\rm t}^{\rm T})$$
$$+ (y_k+\rho\lambda_{k,3})\mathbf{A}_m\mathbf{w}_k + \mathbf{B}(\mathbf{e}_k^{\rm H}+\rho\boldsymbol{\lambda}_{k,\rm e}^{\rm T}). \tag{18c}$$

Then, the problem (14) can be reformulated as

$$\min_{\mathbf{d}_k} \quad \mathbf{d}_k^{\rm H}\beth_k\mathbf{d}_k - 2\text{Re}\left\{\mathbf{z}_k^{\rm H}\mathbf{d}_k\right\}, \tag{19a}$$

$$\text{s.t.} \quad \mathbf{d}_k^{\rm H}\mathbf{d}_k \le m, \forall k \in \mathcal{K}. \tag{19b}$$

Next, we solve this subproblem (19) using the Lagrange dual method. The optimal solution $\mathbf{d}_k^{\rm opt}$ can be given by

$$\mathbf{d}_k^{\rm opt} = (\beth_k + \delta_k\mathbf{I}_M)^{-1}\mathbf{z}_k, \forall k \in \mathcal{K}, \tag{20}$$

where $\delta_k \ge 0$ is the Lagrange multiplier associated with constraint which can be found by bisection search method.

3) Optimizing the Auxiliary Parameters: In this section, we alternately optimize the auxiliary parameters in $\{u_k, v_k, y_k, \mathbf{e}_k, \mathbf{t}_k\}$. These variables can be also solved by the Lagrange multiplier method. Therefore, we can obtain the optimal solution for the these variables as

$$u_k^{\rm opt} = \mathbf{d}_k^{\rm H}\mathbf{A}_k\mathbf{w}_k - \rho\lambda_{k,1} + \mu_k u_k^{(i)}, \forall k \in \mathcal{K}, \tag{21a}$$

$$v_k^{\rm opt} = \frac{\mathbf{d}_k^{\rm H}\mathbf{q} - \rho\lambda_{k,2}}{1+\varrho_k\eta P_{\rm t}^{\rm a}}, \forall k \in \mathcal{K}, \tag{21b}$$

$$y_k^{\rm opt} = \frac{\sum\limits_{m=1,m\neq k}^{K}\mathbf{d}_k^{\rm H}\mathbf{A}_m\mathbf{w}_k - \rho\lambda_{k,3}}{1+\zeta_k\eta}, \forall k \in \mathcal{K}, \tag{21c}$$

$$\mathbf{e}_k^{\rm H} = \frac{\mathbf{d}_k^{\rm H}\mathbf{B} - \rho\boldsymbol{\lambda}_{k,\rm e}^{\rm T}}{1+\chi_k\eta\sigma_1^2}, \mathbf{t}_k^{\rm H} = \frac{\mathbf{d}_k^{\rm H}\mathbf{C} - \rho\boldsymbol{\lambda}_{k,\rm t}^{\rm T}}{1+\varsigma_k\eta\sigma_2^2}, \forall k \in \mathcal{K}, \tag{21d}$$

where $\mu_k, \varrho_k, \zeta_{k,m}, \chi_k, \varsigma_k \ge 0$ are the Lagrange multipliers associated with its corresponding constraint. And the values of these multipliers can be found by the bisection search method.

4) Optimizing the Phase Shifts $\mathbf{\Theta}_1$: We optimize $\mathbf{\Theta}_1$ while fixing the other variables. To simplify the formulation of Problem (14), we first define $\mathbf{T}_1 = x^*\sqrt{P_{\rm t}^{\rm a}}\mathbf{H}_{12}^{\rm H}\mathbf{\Theta}_2^{\rm H}\mathbf{h}_{2u}\mathbf{h}_{b1}^{\rm H}$, $\mathbf{F}_1 \triangleq x^*\sqrt{P_{\rm t}^{\rm a}}\mathbf{h}_{1u}\mathbf{h}_{b1}^{\rm H}$, $\mathbf{S}_k = (\mathbf{H}_{2r}\mathbf{\Theta}_2\mathbf{H}_{12} + \mathbf{H}_{1r})^{\rm H}\mathbf{d}_k(\mathbf{e}_k + \rho\boldsymbol{\lambda}_{k,e})$. $\mathbf{t}_1$, $\mathbf{f}_1$ and $\mathbf{s}_k$ denote the collection of diagonal elements of matrix $\mathbf{T}_1$, $\mathbf{F}_1$ and $\mathbf{S}_k$, respectively. By using the property, $\text{Tr}(\mathbf{\Theta}_1^{\rm H}\mathbf{D}_1\mathbf{\Theta}_1) = \boldsymbol{\phi}_1^{\rm H}(\mathbf{D}_1 \odot \mathbf{I}_{N_1})\boldsymbol{\phi}_1$ and $\text{Tr}(\mathbf{\Theta}_1\mathbf{T}_1^{\rm H}) = \mathbf{t}_1^{\rm H}\boldsymbol{\phi}_1$ in [19], the subproblem can be rewritten as

$$\min_{\boldsymbol{\phi}_1} \quad \boldsymbol{\phi}_1^{\rm H}\mathbf{\Xi}_1\boldsymbol{\phi}_1 - 2\text{Re}\{\mathbf{u}_1^{\rm H}\boldsymbol{\phi}_1\}, \tag{22a}$$

$$\text{s.t.} \quad \boldsymbol{\phi}_1^{\rm H}\mathbf{P}\boldsymbol{\phi}_1 - P_1 \le 0, \tag{22b}$$

$$\boldsymbol{\phi}_1^{\rm H}\mathbf{V}\boldsymbol{\phi}_1 - P_{\boldsymbol{\phi}_1} \le 0, \tag{22c}$$

where the parameters are defined as follow

$$\mathbf{\Xi}_1 = |x|^2\sigma_1^2(\mathbf{h}_{2u}^{\rm H}\mathbf{\Theta}_2\mathbf{H}_{12} + \mathbf{h}_{1u}^{\rm H})^{\rm H}(\mathbf{h}_{2u}^{\rm H}\mathbf{\Theta}_2\mathbf{H}_{12} + \mathbf{h}_{1u}^{\rm H})$$

$$\odot \mathbf{I}_{N_1} + \frac{1}{2\rho}\sum_{k=1}^{K}(\mathbf{b}_k\mathbf{b}_k^{\mathrm{H}} + \mathbf{L}_{1k}), \tag{23a}$$

$$\mathbf{P} = \mathbf{I}_{N_1} \odot (\mathbf{h}_{b1}\mathbf{h}_{b1}^{\mathrm{H}} + \sigma_1^2\mathbf{I}_{N_1})^{\mathrm{T}}, \tag{23b}$$

$$\mathbf{u}_1 = \mathbf{t}_1 + \mathbf{f}_1 - \frac{1}{2\rho}\sum_{k=1}^{K}(\mathrm{m}_k\mathbf{b}_k + \mathbf{s}_k), \tag{23c}$$

$$\mathbf{V} = \mathbf{H}_{12}^{\mathrm{H}}\mathbf{\Theta}_2^{\mathrm{H}}\mathbf{\Theta}_2\mathbf{H}_{12} \odot ((\mathbf{h}_{b1}\mathbf{h}_{b1}^{\mathrm{H}})^{\mathrm{T}} + \sigma_1^2\mathbf{I}_{N_1}), \tag{23d}$$

$$\begin{aligned}\mathbf{L}_{1k} = {} & \sigma_1^2(\mathbf{d}_k^{\mathrm{H}}\mathbf{H}_{2r}\mathbf{\Theta}_2\mathbf{H}_{12} + \mathbf{d}_k^{\mathrm{H}}\mathbf{H}_{1r})^{\mathrm{H}} \\ & \times (\mathbf{d}_k^{\mathrm{H}}\mathbf{H}_{2r}\mathbf{\Theta}_2\mathbf{H}_{12} + \mathbf{d}_k^{\mathrm{H}}\mathbf{H}_{1r}) \odot \mathbf{I}_{N_1},\end{aligned} \tag{23e}$$

$$P_{\boldsymbol{\phi}_1} = P_2 - \|\mathbf{\Theta}_2\mathbf{h}_{b2}\|_2^2 - \sigma_2^2\|\mathbf{\Theta}_2\|_2^2, \tag{23f}$$

$$\mathbf{b}_k^{\mathrm{H}} = \mathbf{d}_k^{\mathrm{H}}(\mathbf{H}_{2r}\mathbf{\Theta}_2\mathbf{H}_{12} + \mathbf{H}_{1r})\mathrm{diag}(\mathbf{h}_{b1}), \tag{23g}$$

$$\mathrm{m}_k = \mathbf{d}_k^{\mathrm{H}}(\mathbf{h}_{br} + \mathbf{H}_{2r}\mathbf{\Theta}_2\mathbf{h}_{b2}) - \upsilon_k - \rho\lambda_{k,2}. \tag{23h}$$

Because $\mathbf{\Xi}_1$, $\mathbf{P}$ and $\mathbf{V}$ are semidefinite matrix, the subproblem (22) is convex. Thus, we can use the Lagrange dual method to get the optimal solution of $\boldsymbol{\phi}_1^{\mathrm{opt}}$, given by

$$\boldsymbol{\phi}_1^{\mathrm{opt}} = (\mathbf{\Xi}_1 + \kappa_1\mathbf{P} + \kappa_2\mathbf{V})^{-1}\mathbf{u}_1, \tag{24}$$

where $\kappa_1, \kappa_2 \geq 0$ are the Lagrange multipliers associated with constraints, which is determined by the ellipsoid method [20].

5) Optimizing the Phase Shifts $\mathbf{\Theta}_2$: We optimize $\mathbf{\Theta}_2$ while fixing the other variables. Firstly, we define $\mathbf{T}_2 \triangleq x^*\sqrt{P_{\mathrm{t}}^{\mathrm{a}}}\mathbf{h}_{2u}\mathbf{h}_{b1}^{\mathrm{H}}\mathbf{\Theta}_1^{\mathrm{H}}\mathbf{H}_{12}^{\mathrm{H}}$, $\mathbf{F}_2 \triangleq x^*\sqrt{P_{\mathrm{t}}^{\mathrm{a}}}\mathbf{h}_{2u}\mathbf{h}_{b2}^{\mathrm{H}}$, $\mathbf{M}_1 \triangleq \sigma_1^2\,|x|^2\,\mathbf{h}_{2u}\mathbf{h}_{1u}^{\mathrm{H}}\mathbf{\Theta}_1\mathbf{\Theta}_1^{\mathrm{H}}\mathbf{H}_{12}^{\mathrm{H}}$, $\mathbf{M}_{2k} \triangleq \mathbf{H}_{2r}^{\mathrm{H}}\mathbf{d}_k\mathbf{d}_k^{\mathrm{H}}\mathbf{H}_{1r}\mathbf{\Theta}_1\mathbf{\Theta}_1^{\mathrm{H}}\mathbf{H}_{12}^{\mathrm{H}}$, $\mathbf{G}_k \triangleq \mathbf{H}_{2r}^{\mathrm{H}}\mathbf{d}_k(\mathbf{t}_k + \rho\boldsymbol{\lambda}_{k,\mathrm{t}})^{\mathrm{H}}$, $\mathbf{Q}_k \triangleq \mathbf{H}_{2r}^{\mathrm{H}}\mathbf{d}_k(\mathbf{e}_k + \rho\boldsymbol{\lambda}_{k,\mathrm{e}})^{\mathrm{H}}\mathbf{H}_{12}^{\mathrm{H}}\mathbf{\Theta}_1^{\mathrm{H}}$. And $\mathbf{t}_2$, $\mathbf{f}_2$, $\mathbf{m}_1$, $\mathbf{m}_{2k}$, $\mathbf{g}_k$, $\mathbf{q}_k$ are the collection of diagonal elements of matrix $\mathbf{T}_2$, $\mathbf{F}_2$, $\mathbf{M}_1$, $\mathbf{M}_{2k}$, $\mathbf{G}_k$ and $\mathbf{Q}_k$, respectively. Thus, this subproblem can be formulated as

$$\min_{\boldsymbol{\phi}_2} \quad \boldsymbol{\phi}_2^{\mathrm{H}}\mathbf{\Xi}_2\boldsymbol{\phi}_2 - 2\mathrm{Re}\{\mathbf{u}_2^{\mathrm{H}}\boldsymbol{\phi}_2\} \tag{25a}$$

$$\text{s.t.} \quad \boldsymbol{\phi}_2^{\mathrm{H}}\mathbf{Z}\boldsymbol{\phi}_2 \leq P_2, \tag{25b}$$

where the parameter are defined as follow

$$\begin{aligned}\mathbf{\Xi}_2 = {} & (|x|^2\,\mathbf{h}_{2u}\mathbf{h}_{2u}^{\mathrm{H}}) \odot (\sigma_1^2(\mathbf{H}_{12}\mathbf{\Theta}_1\mathbf{\Theta}_1^{\mathrm{H}}\mathbf{H}_{12}^{\mathrm{H}})^{\mathrm{T}} + \sigma_2^2\mathbf{I}_{N_2}) \\ & + \frac{1}{2\rho}\sum_{k=1}^{K}(\mathbf{r}_k\mathbf{r}_k^{\mathrm{H}} + \mathbf{L}_{2k}),\end{aligned} \tag{26a}$$

$$\begin{aligned}\mathbf{Z} = {} & \mathbf{I}_{N_2} \odot ((\mathbf{H}_{12}\mathbf{\Theta}_1\mathbf{h}_{b1}\mathbf{h}_{b1}^{\mathrm{H}}\mathbf{\Theta}_1^{\mathrm{H}}\mathbf{H}_{12}^{\mathrm{H}})^{\mathrm{T}} + (\mathbf{h}_{b2}\mathbf{h}_{b2}^{\mathrm{H}})^{\mathrm{T}} \\ & + \sigma_2^2\mathbf{I}_{N_2} + \sigma_1^2(\mathbf{H}_{12}\mathbf{\Theta}_1\mathbf{\Theta}_1^{\mathrm{H}}\mathbf{H}_{12}^{\mathrm{H}})^{\mathrm{T}}),\end{aligned} \tag{26b}$$

$$\mathbf{L}_{2k} = \mathbf{H}_{2r}^{\mathrm{H}}\mathbf{d}_k\mathbf{d}_k^{\mathrm{H}}\mathbf{H}_{2r} \odot ((\mathbf{H}_{12}\mathbf{\Theta}_1\mathbf{\Theta}_1^{\mathrm{H}}\mathbf{H}_{12}^{\mathrm{H}})^{\mathrm{T}} + \mathbf{I}_{N_2}), \tag{26c}$$

$$\mathbf{u}_2 = \mathbf{t}_2 + \mathbf{f}_2 + \mathbf{m}_1 - \frac{1}{2\rho}\sum_{k=1}^{K}(\mathrm{n}_k\mathbf{r}_k + \mathbf{m}_{2k} + \mathbf{g}_k + \mathbf{q}_k), \tag{26d}$$

$$\mathbf{r}_k^{\mathrm{H}} = \mathbf{d}_k^{\mathrm{H}}\mathbf{H}_{2r}(\mathrm{diag}(\mathbf{H}_{12}\mathbf{\Theta}_1\mathbf{h}_{b1}) + \mathrm{diag}(\mathbf{h}_{b2})), \tag{26e}$$

$$\mathrm{n}_k = \mathbf{d}_k^{\mathrm{H}}(\mathbf{h}_{br} + \mathbf{H}_{1r}\mathbf{\Theta}_1\mathbf{h}_{b1}) - \upsilon_k - \rho\lambda_{k,2}. \tag{26f}$$

Then, we can get the optimal solution of $\boldsymbol{\phi}_2^{\mathrm{opt}}$, given by

$$\boldsymbol{\phi}_2^{\mathrm{opt}} = (\mathbf{\Xi}_2 + \xi\mathbf{Z})^{-1}\mathbf{u}_2, \tag{27}$$

where $\xi \geq 0$ is the Lagrange multiplier associated with constraints which is determined by bisection search method.

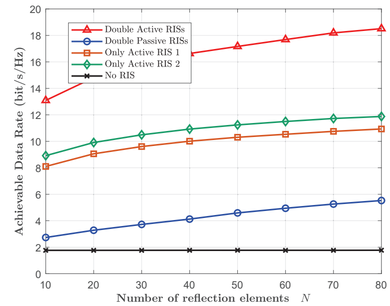

Fig. 2. Achievable data rate versus the total number of reflecting elements.

IV. Simulation Results

In this simulation, we consider a two-dimensional coordinates where the location of BS, UE, active RIS 1, active RIS 2 and radar are set to (0m, 0m), (100m, 0m), (0m, 5 m), (100m, 5m) and (50m, 25m), respectively. The number of reflecting elements of two RISs are $N_1 = N_2 = 40$. The number of antennas for the radar is $M = 12$, and there is $K = 7$ directions which is $[-\pi/2, -\pi/3, -\pi/6, 0, \pi/6, \pi/3, \pi/2]$. The pathloss factors of targets response matrix are $\alpha_k = 10^{-1}, \forall k \in \mathcal{K}$. The radar SINR requirement is set to $\eta = 20$ dB. The large-scale path loss of the channel in dB is considered as $\mathrm{PL} = -30 - 10\alpha\log_{10}(d)$, where α is the large-scale path-loss factor, d is the link distance. We assume the path loss factor $\alpha = 3.75$ for h_{bu} , $\alpha = 2.5$ for $\mathbf{h}_{b1}$ and $\mathbf{h}_{2u}^{\mathrm{H}}$, $\alpha = 3$ for $\mathbf{h}_{b2}$ and $\mathbf{h}_{1u}^{\mathrm{H}}$, $\alpha = 2.2$ for $\mathbf{h}_{br}$, $\mathbf{H}_{1r}$, $\mathbf{H}_{2r}$ and $\mathbf{H}_{12}$. The small-scale fading can be modeled as Rician fading, where Rician factor is set to 3.

To verify the advantages of deploying double active RISs in the RCC system, we mainly compare the following schemes in our simulations: double active RIS, double passive RIS, no RIS, and single active RIS. Then, based on the power model in [8], the total power consumption for the above schemes are described respectively as follows

$$Q^{\mathrm{DAR}} = P_{\mathrm{t}}^{\mathrm{a}} + P_{\mathrm{r}} + P_1 + P_2 + (N_1 + N_2)(P_{\mathrm{S}} + P_{\mathrm{D}}), \tag{28a}$$

$$Q^{\mathrm{DPR}} = P_{\mathrm{t}}^{\mathrm{p}} + P_{\mathrm{r}} + (N_1 + N_2)P_{\mathrm{S}}, Q^{\mathrm{NR}} = P_{\mathrm{t}}^{\mathrm{no}} + P_{\mathrm{r}}. \tag{28b}$$

$$Q^{\mathrm{SAR}} = P_{\mathrm{t}}^{\mathrm{a}} + P_i + P_{\mathrm{r}} + N_i(P_{\mathrm{S}} + P_{\mathrm{D}}), \forall i \in \{1, 2\} \tag{28c}$$

where P_{S}, P_{D} denote the power consumption of the switch and control circuit, the direct current bias power for each active reflecting element, respectively. $P_r = \gamma Q_{\mathrm{total}}$, where $\gamma \in [0, 1]$ is the power allocation factor. Unless specified otherwise, we set $Q_{\mathrm{total}} = 11$ W, $P_{\mathrm{SW}} = -10$ dBm, $P_{\mathrm{DC}} = -5$ dBm, $P_{\mathrm{t}}^{\mathrm{a}} = P_1 = P_2$, $\gamma = 0.9$. Specifically, we compare the performance difference between these schemes with the same total power budget and the same total number of reflecting elements of RISs for fairness.

Fig. 2 compares the achievable data rate versus the number of reflecting elements. Note that the total number of elements $N = N_1 + N_2$ is the same for different schemes. Fig. 2 shows that the data rate of the double active RIS-assisted system can significantly outperform the other benchmarks. It illustrates

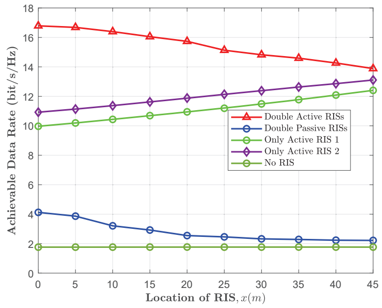

Fig. 3. Achievable data rate versus locations of RIS, $x(m)$.

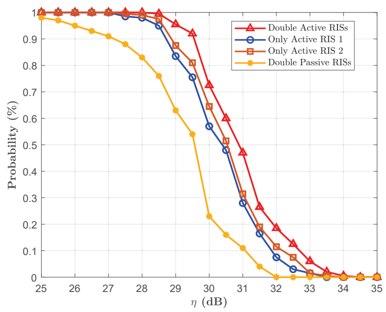

Fig. 4. Successful probability of a feasible solution versus η.

that active RIS can effectively overcome the link "multiplicative fading" effect introduced by passive RIS. Meanwhile, the double active RIS-assisted RCC system performs better than the single active RIS-assisted RCC system.

In Fig. 3, we investigate the impact of the locations of two RISs on the achievable data rate by moving the positions of two RISs. By denoting the horizontal coordinate of the RIS 1 as x, the locations of RIS 1 and RIS 2 are set to (x m, 0 m), ($100 - x$ m, 0 m), respectively. It can be seen that the double active RIS-assisted system has superior performance than other schemes in all locations. Furthermore, double RISs can be regarded as a single RIS equipped with $N_1 + N_2$ reflecting elements as the two RISs get closer to each other, which is consistent with the phenomenon in Fig. 3.

In Fig. 4, we study the successful probability of a feasible solution versus radar SINR requirements, i.e., η. As η increases, it becomes more difficult to find a feasible solution that satisfies radar SINR requirements. It shows that a double active RIS-assisted system finds a feasible solution more easily than the other schemes for the same η. It demonstrates that double active RISs can more effectively reduce the interference from communication systems to radar.

V. Conclusions

In this paper, we have investigated the double active RIS-assisted RCC system. We formulated a achievable data rate maximization problem with the guaranteed radar SINR requirement and the power budget limitations of the radar and two active RISs. Because of the nonconvexity of the original problem, we used the FP method and CCP method based on PDD framework to convert the original problem to a convex problem. Then, we used BCD method to obtain the optimal solution of each variable. Simulation results verified the proposed algorithm achieves higher system performance than other benchmark schemes under the same power budget and number of reflecting elements.

Acknowledgment

The work of Cunhua Pan was supported in part by the National Natural Science Foundation of China under Grants 6504009731, 62201137, 62350710796 and 62331023.

References

[1] F. Liu, C. Masouros *et al.*, "Joint radar and communication design: Applications, state-of-the-art, and the road ahead," *IEEE Trans. Commun.*, vol. 68, no. 6, pp. 3834–3862, 2020.

[2] M. Labib, V. Marojevic, A. F. Martone, J. H. Reed, and A. I. Zaghloui, "Coexistence between communications and radar systems: A survey," *URSI Radio Sci. Bull.*, vol. 2017, no. 362, pp. 74–82, 2017.

[3] L. Zheng, M. Lops, Y. C. Eldar, and X. Wang, "Radar and communication coexistence: An overview: A review of recent methods," *IEEE Signal Process. Mag.*, vol. 36, no. 5, pp. 85–99, 2019.

[4] X. Wang, Z. Fei, J. Guo, Z. Zheng, and B. Li, "RIS-assisted spectrum sharing between MIMO radar and MU-MISO communication systems," *IEEE Wireless Commun. Lett.*, vol. 10, no. 3, pp. 594–598, 2020.

[5] Y. He, Y. Cai, H. Mao, and G. Yu, "RIS-assisted communication radar coexistence: Joint beamforming design and analysis," *IEEE J. Sel. Areas Commun.*, vol. 40, no. 7, pp. 2131–2145, 2022.

[6] C. Pan, H. Ren *et al.*, "Multicell MIMO communications relying on intelligent reflecting surfaces," *IEEE Trans. Wireless Commun.*, vol. 19, no. 8, pp. 5218–5233, 2020.

[7] Z. Zhang, L. Dai, X. Chen, C. Liu, F. Yang, R. Schober, and H. V. Poor, "Active RIS vs. passive RIS: Which will prevail in 6G?" *IEEE Trans. Commun.*, vol. 71, no. 3, pp. 1707–1725, 2022.

[8] K. Zhi, C. Pan, H. Ren, K. K. Chai, and M. Elkashlan, "Active RIS versus passive RIS: Which is superior with the same power budget?" *IEEE Commun. Lett.*, vol. 26, no. 5, pp. 1150–1154, 2022.

[9] Q. Zhu *et al.*, "Joint transceiver beamforming and reflecting design for active RIS-aided ISAC systems," *IEEE Trans. Veh. Technol.*, 2023.

[10] A. A. Salem, M. H. Ismail, and A. S. Ibrahim, "Active reconfigurable intelligent surface-assisted MISO integrated sensing and communication systems for secure operation," *IEEE Trans. Veh. Technol.*, 2022.

[11] A. L. Swindlehurst, G. Zhou, R. Liu, C. Pan, and M. Li, "Channel estimation with reconfigurable intelligent surfaces—a general framework," *Proc. IEEE*, vol. 110, no. 9, pp. 1312–1338, 2022.

[12] B. Zheng, C. You, and R. Zhang, "Efficient channel estimation for double-irs aided multi-user mimo system," *IEEE Transactions on Communications*, vol. 69, no. 6, pp. 3818–3832, 2021.

[13] L. Zheng, M. Lops, and X. Wang, "Adaptive interference removal for uncoordinated radar/communication coexistence," *IEEE J. Sel. Topics Signal Process.*, vol. 12, no. 1, pp. 45–60, 2017.

[14] A. Khawar *et al.*, "Spectrum sharing between S-band radar and LTE cellular system: A spatial approach," in *Proc. IEEE Int. Symp. Dynamic Spectrum Access Networks (DYSPAN)*. IEEE, 2014, pp. 7–14.

[15] K. Shen and W. Yu, "Fractional programming for communication systems—Part I: Power control and beamforming," *IEEE Trans. Signal Process.*, vol. 66, no. 10, pp. 2616–2630, 2018.

[16] A. L. Yuille and A. Rangarajan, "The concave-convex procedure," *Neural Comput.*, vol. 15, no. 4, pp. 915–936, 2003.

[17] Q. Shi and M. Hong, "Penalty dual decomposition method for nonsmooth nonconvex optimization—Part I: Algorithms and convergence analysis," *IEEE Trans. Signal Process.*, vol. 68, pp. 4108–4122, 2020.

[18] D. P. Bertsekas, "Nonlinear programming," *J. Oper. Res. Soc.*, vol. 48, no. 3, pp. 334–334, 1997.

[19] X.-D. Zhang, *Matrix analysis and applications*. Cambridge Univ. Press, 2017.

[20] S. Boyd and Z. Luo, "EE392o: Optimization projects," Available: http://www.stanford.edu/class/ee392o, 2004.